Nano-Displacement Measurement using an Optical Drop-shaped Structure

Paulo Robalinho, Orlando Frazão

***Abstract*— This letter presents a new optical fiber structure with the capability of measuring nano-displacement. This device is composed by a cleaved fiber and a drop-shaped microstructure that is connected to the fiber cladding. This optical structure is responsible for the light beam division and the formation of new optical paths. The operation mode consists of the Vernier effect that allows achieving higher sensitivity than the currently sensors. During the experimental execution, displacement sensitivities of 1.05 ± 0.01 nm/µm, 15.1 ± 0.1 nm/µm, 24.7 ± 0.3 nm/µm and 28.3 ± 0.3 nm/µm, were achieved for the carrier, the fundamental of the envelope, the first harmonic and the second harmonic, respectively. The *M*-factor of 27 was attained, allowing a minimum resolution of 0.7 nm. In addition to displacement sensing, the proposed optical sensor can be used as a cantilever enabling non-evasive measurements.**

***Index Terms*— Optical microstructure, optical fiber tip, micrometric displacement, optical microsphere, optical fiber sensor, displacement optical sensor**

I. Introduction

THE first glass optical fiber appeared in the 1960s [1]. This invention allowed the application of optics in various fields such as: light sources, sensors, and communications. The first great achievement of the optical fiber was to have replaced the electric coaxial cable due to its low attenuation, which allowed the transmission of a signal over long distances, besides its low-cost production. In addition, the insensitivity of fiber optics to electromagnetic fields allowed the design of sensors with applicability in micro and nano manufacturing as well as for determining the states of micro and nano systems.

At the end of the 20th century to the present day, several fiber sensors appeared. The simplest of them is the cleaved fiber tip [2] that allows the conception of sensors in intensity or, if they are coupled to a mirror, interferometric sensors. The fiber sensors with the highest applicability until now are FBGs (Fiber Bragg Gratings) [3] and LPGs (Long-Period Fiber Grating) [4]. Furthermore, optical microstructures such as tapers [5] and microspheres [6] have produced high interest after the improvement of micro and nano fabrication. The taper consists of a narrow optical fiber (which can have conical or cylindrical geometry) allowing a larger evanescent field. Thus, the optical signal is subjected to a higher interaction with external environment. It is also an excellent way to select optical modes to be coupled between different optical structures. Microspheres are usually produced by CO_2 laser or by electric arc at the tip of the optical fiber. Currently, the study of these optical structures focuses on large microspheres or in its application to tapers. Optical microstructures also have a key role in the implementation of Whisper Gallery Modes (WGM) for sensing [7].

So far, several displacement sensors have been developed, presenting a wide range of sensitivities. For large ranges, LPGs FBGs and Mach-Zehnder may present sensitivities of 0.22 nm/µm [8], 0.62 nm/mm [9] and 1.53 nm/ µm [10], respectively. For narrow ranges, the application of SPR (Surface Plasmon resonance) has also been used to increase the displacement sensitivity and values of 10.32 nm/ µm [11] and 31.45 nm/nm [12] have already been achieved, however in short range measurement.

Recently, the Vernier effect has been applied for the achievement of giant sensitivities in optical sensing. The first interferometric optical sensor based on the Vernier effect appeared in 2011 [13], followed by several applications. This effect consists in the generation of two waves, the envelope, and the carrier, based on the overlapping of the interferometric fringes of two cavities, that is, a spectral beat. In this effect, the envelope is typically used because it reveals a higher sensitivity than the carrier.

In this research, a new optical microstructure developed at the fiber tip is explored for sensing. This structure is fused to the optical fiber cladding presenting a drop-shaped geometry. For the purpose of displacement sensing, the operation mode consists in creating two optical cavities: the reference (generated by the drop-shaped structure) and the sensing cavity. The output light (optical fiber core) is divided into two beams, one goes to the optical drop and the other to a reflective surface. The light is then reflected by the reflecting surface and it is re-coupled into the fiber core thus forming the sensing cavity. Therefore, three optical paths interfere with each other, giving rise to the Vernier effect [14]. Although there are several studies on cleaved tips that use the Vernier effect with multiple optical cavities [15], the proposed sensor uses only two optical cavities to avoid unwanted phenomena. This optical microstructure has several applications where the main one is for displacement sensing. It is also measured in reflection, i.e. no mechanical

This work is financed by National Funds through the Portuguese funding agency, FCT - Fundação para a Ciência e a Tecnologia, within project UIDB/50014/2020.

P. Robalinho (e-mail: paulo.robalinho@inesctec.pt) and O. Frazão (e-mail: ofrazao@inesctec.pt) are with INESC TEC, Rua do Campo Alegre 687, 4169-007 Porto, Portugal

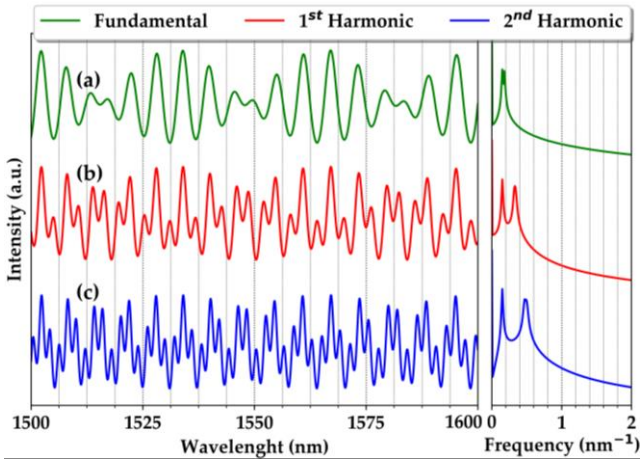

Fig. 1: Vernier effect simulation for two cavities: (a) Fundamental with 505 µm and 605 µm, (b) 1st Harmonic with 505 µm and 1110 µm and (c) 2nd Harmonic with 505 µm and 1615 µm; the signals and their FFT are shown.

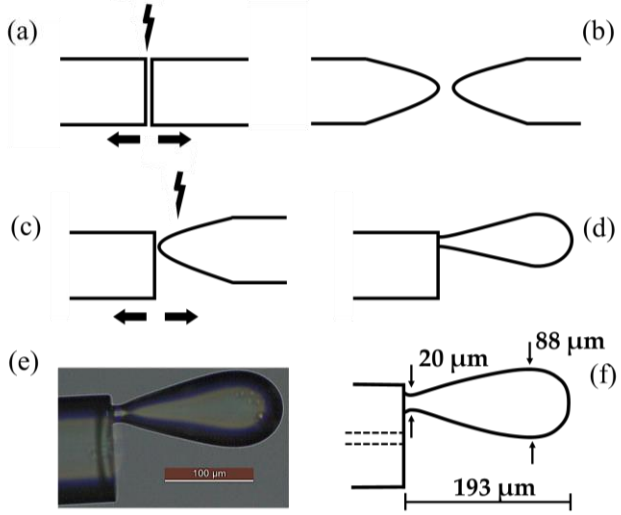

Fig. 2: Manufacture step of the optical drop at the fiber tip (a-d), microscopic image of the drop-shaped sensor structure (e), and its dimensions (f).

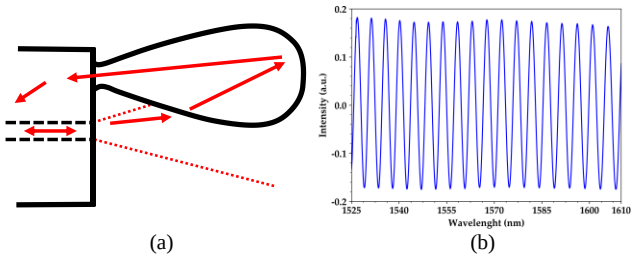

Fig. 3: Drop-shaped sensor structure (a) internal cavity scheme and (b) optical spectrum.

coupling is required to the system under evaluation, allowing non-evasive measurements in addition to requiring less space.

II. Theorical Considerations

The phenomenon of two optical waves beating is widely known. It consists of the overlap of two optical waves leading to the creation of two new optical wave whose frequencies are: the difference of the optical wave's frequency, named envelope, and a wave whose frequency is the sum of the wave's frequencies, named carrier. However, this phenomenon also exists in interferometry and can be obtained by the overlapping of two interferences, that is, by the signal overlapping of two optical cavities, i.e., the sensing and the reference cavities. This phenomenon is named the Vernier effect [16]. This effect has as dimension the wavelength. Furthermore, in the optical domain, the distance between successive extremes is smaller for shorter wavelengths, that is, the spectral frequency depends on the wavelength unlike sound waves whose frequency is constant over time. Considering that the sensing and the reference cavities are Fabry-Perot interferometers, the distance between two consecutive maxima (FSR) can be obtained as follows:

$$\beta L = 2\pi m \tag{1}$$

where β is the wavenumber, L the cavity length and m the order of maximum.

Then results the following expression:

$$m = \frac{nL}{\lambda} \Longrightarrow \Delta m = \frac{nL}{\lambda^2}\Delta\lambda \tag{2}$$

Therefore, FSR ($\Delta\lambda$) is obtained when Δm = 1, that is, consecutive maxima:

$$\Delta\lambda = \frac{\lambda^2}{nL} \tag{3}$$

where n is the refractive index.

The equation that allows to describe the fringes resulting from the interference between two optical paths can be described by:

$$I = A\cos\left(\frac{\pi}{\lambda}nL\right) + I_o \tag{5}$$

where I_o the difference in intensity between the optical paths.

So, the Vernier effect can be written as follows:

$$I = 2\cos\left(\frac{\pi}{2\lambda}[n_1L_1 - n_2L_2]\right)\cos\left(\frac{\pi}{2\lambda}[n_1L_1 + n_2L_2]\right) + I_0 \tag{6}$$

where n_1L_1-n_2L_2 is associated to the envelope and n_1L_1+n_2L_2 is associated to the carrier. Fig. 1 presents the simulation results where is considered a refractive index of 1.44. For this, a 505 µm reference cavity is used. Thus, if the sensing cavity (605 µm) has a dimension close to the reference cavity, the fundamental wave of the Vernier effect is enabled. If the dimension of the sensing interferometer is close to double (1110 µm), then the 1st harmonic appears and if the dimension is the triple (1615 µm), the 2nd harmonic is generated. The efficiency of the Vernier effect implementation is a relevant issue to determine the optimization of the system. In this effect, the objective is to use the envelope because it reveals a higher sensitivity than the carrier's sensitivity. The magnification factor (M factor) can be calculated when higher envelope and lower carrier sensitivities are shown, which is described as follows [17]:

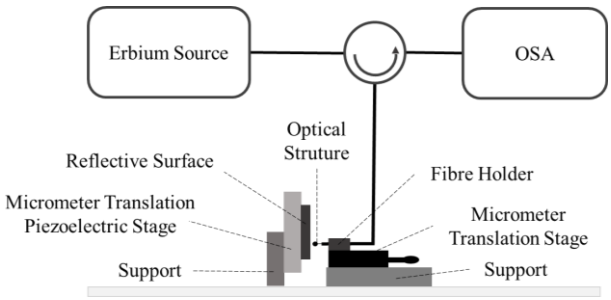

Fig. 4: Setup used for nano-scale measurement.

$$M = \frac{Sens_{env}}{Sens_{carr}}. \quad (7)$$

III. Fabrication and Operation Mode

The drop-shaped microstructure manufacturing process is described in Fig. 2. Firstly, a tension is applied simultaneously in the fusion process between two cleaved single mode fibers (SMF28) (Fig. 2.a), resulting in two tapers (Fig. 2.b). The electrical arc features are: -100 a.u. of power and 10 s of duration. Then, a taper is fused to a cleaved fiber and simultaneously a tension is applied on the taper (Fig. 2.c) giving rise to the proposed drop-shaped structure (Fig. 2.d). The electric arc is applied on the taper and its characteristics are: -100 a.u. of power and 4 s of duration. This drop-shaped microstructure was produced using a conventional splice machine ("Sumitomo Electric— Type-72C", Osaka, Japan). The microscopic image of the drop-shaped structure is depicted in Fig. 2.e and it has the following dimensions (Fig.2.f): 193 µm -length, 88 µm-width and a 20 µm-junction. From Fig.3, it was estimated that the reference cavity consists of an air path with a length of 73 µm and a path inside the drop-shaped microstructure with a length of 300 µm. Thus, it implies that the fringes associated with the reference cavity have a width of 4.8 nm which is demonstrated in the internal cavity spectrum (Fig. 3.b).

The displacement sensor mode of operation consists of dividing the light beam through the optical drop-shaped microstructure and the reflective surface. The reference cavity is formed by the drop-shaped structure and the sensing cavity is obtained by the optical path between the cleaved optical fiber and the reflective surface. In this case, the optical path is in the air and when the sensing structure is displaced the pattern fringe changes. The combination of the two pattern fringes form a beat signal.

IV. Experimental Setup and Results

Fig. 4 presents the experimental scheme that was used to test the displacement sensor. It consists of a broadband source centered at 1570 nm and 90 nm-bandwidth, and an optical spectrum analyzer (OSA) ("Advantest Q8384") with a resolution of 0.02 nm. A reflective surface is also used, and it is coupled to a piezoelectric with a displacement of 32.8 ± 0.2 nm/V.

The displacement sensor is characterized for nano-displacements using the piezoelectric component. To obtain the beats (envelope and harmonics), different distances were used

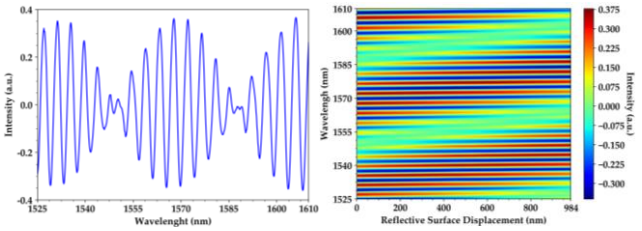

(a) (b)

Fig. 5: Output signal for the fundamental beat: (a) initial spectrum and (b) intensity as a function of wavelength and the distance between the sensor and the reflective surface.

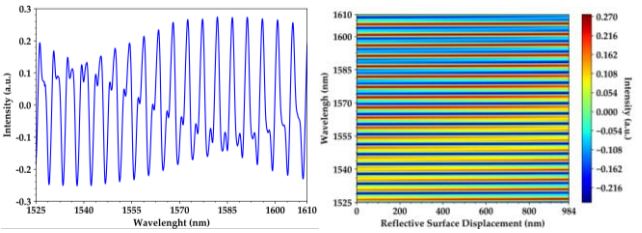

(a) (b)

Fig. 6: Output signal for the 1st harmonic: (a) initial spectrum and (b) intensity as a function of wavelength and the distance between the sensor and the reflective surface.

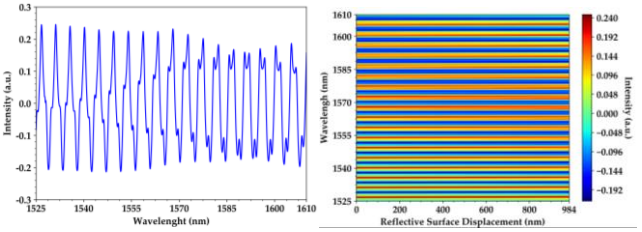

(a) (b)

Fig. 7: Output signal for the 2nd harmonic: (a) initial spectrum and (b) intensity as a function of wavelength and the distance between the sensor and the reflective surface.

between the first reflection of the fiber and the reflective surface. The length of the sensing cavity is 252.5 µm, given by the envelope signal, which is obtained by the distance between the drop-shaped microstructure and the reflective surface. In terms of an optical path it is equivalent to the reference cavity.

To obtain harmonics, the length of the sensing cavity must be changed to double or triple the initial length (252.5 µm) of the envelope signal. To obtain maximum sensitivities for both the envelope and the harmonics, it is necessary to place the sensor cavity close to the reference cavity or by a multiple value of it.

Then follows the analysis of the sensitivity of each state of the environment. The envelope and carrier fringe of each matrix were extracted (Fig. 5.b, 6.b, and 7.b) being independently analyzed. In Fig. 5.a) is presented the spectrum at the beginning of the measurements and Fig. 5.b) the spectral variation with the reflective surface displacement. The envelope sensitivity is 15.1 ± 0.1 nm/µm with an r^2 of 0.9992 resulting in a *M*-factor of 14 (see Fig. 8). If the sensing cavity is similar to the double of the reference cavity, the first harmonic appears, and it is observed in Fig.6. The envelope sensitivity is 24.7 ± 0.3 nm/µm with an r^2 of 0.997 resulting in a *M*-factor of 24 (see Fig. 7). For a length that is triple of the reference cavity, the second harmonic is generated (see Fig. 8). In this case, the sensor

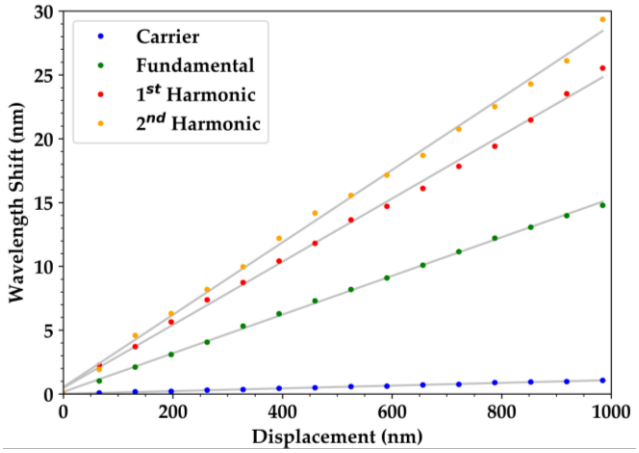

Fig. 8: Wavelength shift for Carrier and Envelopes (Fundamental, 1st Harmonic and 2nd Harmonic

presents a maximum envelope sensitivity with 28.3 ± 0.3 nm/µm and r^2 of 0.997 resulting in a *M*-factor of 27. With this new sensor, the maximum sensitivity using the second harmonic is three-fold the sensitivity of SPR sensors [12]. Considering that the 2nd harmonic was observed, then the dynamic range verified is 760 µm.

Fig. 8 presents the slopes of the envelope and harmonics, as well as the carrier, as it shows the lowest sensitivity of 1.05 ± 0.01 nm/µm and r^2 of 0.997. Summarizing, the second harmonic presents the best sensitivity result, being double the sensitivity of the envelope.

V. Conclusion

This work demonstrated that the optical fiber drop-shaped microstructure provides a micrometric range displacement sensor with higher sensitivity than the present optical sensors. Also, the proposed structure allows obtaining the different harmonics of Vernier's effect unlike the structures described in the current literature. The carrier has a sensitivity of 1.05 ± 0.01 nm/µm and in the envelope's fundamental, the sensitivity obtained was of 15.1 ± 0.1 nm/µm. For the first harmonic, the sensitivity obtained was 24.7 ± 0.3 nm/µm and for the second harmonic 28.3 ± 0.3 nm/µm with an *M*-factor of 27. Considering the minimum resolution of the OSA (0.02 nm), the lowest displacement resolution of this optical system is 0.7 nm.

Another possible application of this sensor is to use a flexible reflective surface which, based on the measurement of the surface micro-curvature, it is possible to determine the micro-force applied to the surface. If the dimensions of the microstructure increase, it will give a higher sensitivity allowing the determination of molecular oscillations. One of the advantages of this sensor is that there is no contact with the system being measured, allowing a non-evasive sensing. This characteristic is very useful for biological microsystems as well as for the manufacture of micro and nanostructures.

References

[1] L. T. Krolak, W. P. Siegmund, R. G. Neuhauser, "Fiber Optics - A New Tool in Electronics", SMPTE, 1960, vol. 69, no. 10, doi: 10.5594/J09399.

[2] O. Frazão, S. O. Silva, J. Viegas, L. A. Ferreira, F. M. Araújo, J. L. Santos, "Optical fiber refractometry based on multimode interference", APPLIED OPTICS, 2011, vol. 50, no. 25, doi: 10.1364/AO.50.00E184

[3] O. Xu, J. Zhang, H. Deng, J. Yao, "Dual-frequency Optoelectronic Oscillator forThermal-Insensitive Interrogationof a FBG Strain Sensor", IEEE Photonics Technology Letters, 2017, vol. 29, iss. 4, pp. 357-360, doi: 10.1109/LPT.2016.2647261

[4] D. Barrera, J. Madrigal, S. Sales, "Long Period Gratings in Multicore Optical Fibers for Directional Curvature Sensor Implementation", Lightwave Technology, 2018, vol. 36, iss.4, pp. 1063-1068, doi: 10.1109/JLT.2017.2764951

[5] K. Ni, T. Li, L. Hu, W. Qian, Q. Zhang, S. Jin, "Temperature-independent curvature sensor based on tapered photonic crystal fiber interferometer", Optics Communications, 2012, vol. 285, iss. 24, pp. 5148-5150, doi: 10.1016/j.optcom.2012.08.037

[6] M. S. Ferreira, J. L. Santos, O. Frazão, "Silica microspheres array strain sensor", Optics Letters, 2014, vol. 39, iss. 20, pp.5937-5940, doi: 10.1364/OL.39.005937

[7] R. Boeck, N. A. F. Jaeger, N. Rouger, L. Chrostowski, "Series-coupled silicon racetrack resonators and the Vernier effect: theoryand measurement", Optics Express, 2010, vol. 18, no. 24, pp. 25151-25157, doi: 10.1364/OE.18.025151

[8] L. Qi, C.-L. Zhao, Y. Wang, J. Kang, Z. Zhang, S. Jin, "Compact micro-displacement sensor with high sensitivity based on a long-period fiber grating with an air-cavity", Optics Express, 2013, vol. 21, iss. 3, pp. 3193-3200, doi: 10.1364/OE.21.003193

[9] J. Hong Ng, X. Zhou, X. Yang, J. Hao, "A simple temperature-insensitive fiber Bragg grating displacement sensor", Optics Communications, 2007, vol. 273, iss. 2, pp. 398-401, doi: 10.1016/j.optcom.2007.01.040

[10] J. Chen, J. Zhou, X. Yuan, "M–Z Interferometer Constructed by Two S-Bend Fibers for Displacement and Force Measurements", IEEE Photonics Technology Letters, 2014, vol. 26, iss. 8, pp. 837-840, doi: 10.1109/LPT.2014.2308327

[11] Z. Zhu, L. Liu, Z. Liu, Y. Zhang, Y. Zhang, "High-precision micro-displacement optical-fiber sensor based on surface plasmon resonance", Optics Letters, 2017, vol.42, no. 10, doi: 10.1364/OL.42.001982

[12] X.-M. Wang, C.-L. Zhao, Y.-R. Wang, C.-Y. Shen, X.-Y. Dong, "A Highly Sensitive Fibre-Optic Nano-Displacement Sensor Based on Surface Plasmon Resonance", IEEE, 2016, vol. 34, iss. 9, pp. 2324-2330, doi: 10.1109/JLT.2016.2535662

[13] X. Zhang, L. Ren, X. Wu, H. Li, L. Liu, L. Xu, "Coupled optofluidic ring laser for ultrahigh- sensitive sensing", Optics Express, vol. 19, iss. 22, pp. 22242 – 22247, Oct. 2011, DOI: 10.1364/OE.19.022242.

[14] J. Li, M. Zhang, M. Wan, C. Lin, S. Huang, C. Liu, Q. He, X. Qiu, X. Fang, "Ultrasensitive refractive index sensor based on enhanced Vernier effect through cascaded fiber core-offset pairs", Optics Express, 2020, vol. 28, iss. 3, pp. 4145-4155, doi: 10.1364/OE.384815

[15] E. V.-Rodriguez, A. D. G.-Chavez, R. Baeza-Serrato, M. A. G-Ramirez, "Optical Fiber FP Sensor for Simultaneous Measurement of Refractive Index and Temperature Based on the Empirical Mode Decomposition Algorithm", Sensors, 2020, vol. 20, iss. 3, no. 664, doi: 10.3390/s20030664.

[16] A. D. Gomes, M. S. Ferreira, J. Bierlich, J. Kobelke, M. Rothhardt, H. Bartelt, O. Frazão, "Optical Harmonic Vernier Effect: A New Tool for High Performance Interferometric Fiber Sensors", Sensors, 2019, vol. 19, iss. 24, no. 5431, doi: 10.3390/s19245431

[17] P. Robalinho, A. Gomes, O. Frazão, "High Enhancement Strain Sensor Based on Vernier Effect Using 2-Fiber Loop Mirrors", IEEE, 2020, vol. 32, iss. 18, pp. 1139-1142, doi: 10.1109/LPT.2020.3014695